Application of a full-order extended Luenberger observer for a position sensorless operation of a switched reluctance motor drive

Ç.Elmas
H.Zelaya-De La Parra

Indexing terms: Switched reluctance motor, Extended Luenberger observer

Abstract: Switched reluctance motors (SRMs) are rapidly becoming more popular in industrial applications where variable speed is required because of their simple construction, ease of maintenance, low cost and high efficiency. However, the operation of the SRM is heavily dependent upon precise information about rotor position, measurement of which may be very expensive or prohibited because of the nature of the application. The paper investigates the use of observer theory to eliminate the problems of having to measure the rotor position. For this purpose, observer algorithms based upon the extended Luenberger observer theory have been developed. These include plant nonlinearities which naturally lead to an estimator with improved performance over the existing estimation schemes. To verify the effectiveness of the proposed algorithm, both theoretical study and practical implementation were done and satisfactory results were obtained.

List of symbols

$\mathbf{A}$, $\mathbf{B}$, $\mathbf{C}$ = coefficient matrixes
D = damping coefficient
$\mathbf{e}(t)$ = dynamics of the estimation errors term
$\mathbf{I}$ = identity matrix
J = total inertia
$\mathbf{K}$ = observer matrix
$\mathbf{L}(\theta)$ = phase inductance
$\mathbf{L}_{a,b,c,d}$ = phase inductance
$\mathbf{R}_{a,b,c,d}$ = phase resistances
T, T_e = motor electrical torque
T_L = motor load torque
$\mathbf{u}$ = known input vector
V = DC source voltage
$\mathbf{y}$ = measured output vector
$\hat{x}$ = estimated value of variable x
$\check{\mathbf{A}}$ = state matrix of the linear part of the Taylor expansion
$\check{x}$ = variable x on which Taylor expansion is made
θ = rotor position
ω = angular speed of the motor
ψ = flux linkage

Subscripts

$_N$ = augmented or original
$_P$ = related to motor parameter

Superscripts

^{T} = transpose of a matrix

IEE Proceedings online no. 19960421

Paper first received 26th May 1995 and in final revised form 19th February 1996

H. Zelaya-De La Parra is with the School of Electronic and Electrical Engineering, University of Birmingham, Birmingham. B15 2TT

Dr Elmas is now with the Gazi University, Besevler, Ankara, Turkey

1 Introduction

The switched reluctance motor (SRM) has obtained an increasing interest in electric drive applications because of their robust mechanical construction and reduced rotor losses. The manufacturing cost of the SRM is relatively low when compared to its PM brushless or induction motor counterparts and the simplicity of its associated drive gives increased reliability [1].

When the appropriate phases are energised, the torque developed by the SRM is heavily dependent on the rotor position. Thus torque control of an SRM drive needs accurate knowledge of the rotor position to perform an effective current control. To this purpose the SRM motors are usually equipped with a shaft encoder or a resolver. There are various drawbacks associated with conventional sensors, for instance, limited speed range and poor performance at low frequencies is a common problem.

The desire of eliminating the need of using position sensor has stimulated the research towards the use of methods to determine the rotor position without a mechanical position encoder or a resolver. The methods used so far can be classified into two parts: indirect position sensing and estimation of rotor position from the terminal quantities of the motor.

Considerable improvements in controlling the dynamics of an SRM without using a mechanical position sensor were achieved in early 1980s [2–4], and still the subject of research [5, 6]. The idea behind this method is to determine the position of the rotor by using inductance or mutual inductance effects. An

extensive review of this particular position sensorless control schemes for a switched reluctance drive (SRD) can be found in a recent paper [7]. So far, however, only a few schemes have been reported on the use of an estimator or observer for the sensorless operation of the SRD [8, 9].

In recent years there has been a vast amount of research devoted to the application of estimator or observer in many different types of drives e.g. induction motor [10], brushless DC motor [11]. In SRD field, the application of observer theory first reported in [8] in which the system was considered as a linear dynamic model and a deterministic observer by means of a Lyapunov function was applied. The assumption of the linear dynamic model has resulted in omitting the time dependence of the rotation speed. Consequently, the performance of the observer was poor during transients. In [9] this problem was addressed and a solution together with the practical results was presented based on a reduced-order extended Luenberger observer (ROELO). However, since the model does not cover all states of the system it is expected that the observer is sensitive to the parameter variations and noise. Therefore, it would only be suitable for relatively low dynamic performance [9].

Since the full-order observer covers all system states, its eigenvalues are theoretically equal to those of the actual system. In this way, the dynamic behaviour of the observer error response is the same as that of the underlying system. However, the full-order observer should be designed such that fast convergence rates can be achieved with reduced sensitivity to motor parameter variations [12].

This paper reports a systematic approach for the application of a full-order extended Luenberger observer (FOELO) algorithms based upon a nonlinear machine model that allows for the coupling of mechanical and electrical modes.

2 Luenberger observer

The theory of state estimation from measured data dates back to the early 1960s. The problem of estimating a linear function of the state was considered by Luenberger [13] in the realm of single-output linear systems. He addresses the problem of a reduced observer. The predictor was first obtained by Kalman [14], known as the Kalman filter (KF), and provides estimation for linear systems.

The Luenberger observer (LO) provides solutions for linear systems assuming the system matrix is constant and the parameters do not vary. In practice, however, parameter variation does usually exist with time and the system cannot be considered as linear time-invariant.

As some of the state variables $\mathbf{x}(t)$ are not directly measurable, they have to be determined using measurable quantities. Consider a linear time-invariant system as:

$$\dot{\mathbf{x}}(t) = \mathbf{A}\mathbf{x}(t) + \mathbf{B}\mathbf{u}(t) \tag{1}$$

$$\mathbf{y}(t) = \mathbf{C}\mathbf{x}(t) \tag{2}$$

where dim $x = n$, dim $y = m$, $m \leq n$ and dim $u = r$.

Where we assume that only the input vector $\mathbf{u}(t)$ and output vector $\mathbf{y}(t)$ can be measured without error and the state variables $\mathbf{x}(t)$ are completely observable.

Following [15], if the states are donated the estimate of $\mathbf{x}(t)$ by $\hat{\mathbf{x}}(t)$ then for a linear time-invariant system, the observer is defined as:

$$\dot{\mathbf{z}}(t) = \mathbf{F}\mathbf{z}(t) + \mathbf{K}\mathbf{y}(t) + \mathbf{H}\mathbf{u}(t) \tag{3}$$

here dim $z = n - h$. If a complete model of the process is applied, the observer becomes an 'identity observer' or a 'full-order observer'. If some of the state are available and do not need to be estimated then it is called a 'reduced-order observer'. If $\mathbf{H} = 0$ then the observer is of full-order and in this case $\mathbf{z}(t) = \hat{\mathbf{x}}(t)$ and the observer becomes:

$$\dot{\hat{\mathbf{x}}} = \mathbf{A}\hat{\mathbf{x}}(t) + \mathbf{B}\mathbf{u}(t) + \mathbf{K}(\mathbf{y}(t) - \hat{\mathbf{y}}(t)) \tag{4}$$

$$\hat{\mathbf{y}}(t) = \mathbf{C}\hat{\mathbf{x}}(t) \tag{5}$$

where the estimation error is generated by feeding back the difference between states and the estimated states

$$\mathbf{e}(t) = \mathbf{x}(t) - \hat{\mathbf{x}}(t) \tag{6}$$

and with eqns. 1 and 4 it follows that:

$$\dot{\mathbf{e}}(t) = \underbrace{[\mathbf{A} - \mathbf{K}\mathbf{C}]}_{F}\mathbf{e}(t) \tag{7}$$

which implies that, regardless of the initial conditions and input, the error approaches zero asymptotically as $t \rightarrow \infty$ provided that the eigenvalues of gain matrix $\mathbf{F}$ are located in the left of the complex frequency plane [16].

3 Modelling a switched reluctance motor

The augmented motor model can be shown in a state space representation [17, 18] of the machine equations as:

$$\frac{d\psi}{dt} = -\mathbf{R}\mathbf{L}^{-1}(\theta)\psi + \mathbf{v} \tag{8}$$

$$\frac{d\omega}{dt} = \frac{T - T_L}{J} - \frac{D}{J}\omega \tag{9}$$

$$\frac{d\theta}{dt} = \omega \tag{10}$$

and

$$T = \sum_{n=1}^{4} \frac{1}{2} i_n^T \frac{\partial \mathbf{L}_n(\theta)}{\partial \theta} i_n \tag{11}$$

where $\mathbf{v} = [v_a, v_b, v_c, v_d]^T$ is the terminal voltage vector, $\mathbf{i} = [i_a, i_b, i_c, i_d]^T$ is the phase current vector, and $\psi = [\psi_a, \psi_b, \psi_c, \psi_d]^T$ is the flux linkage vector. $\mathbf{R}$ is the diagonal matrix of phase resistance.

From the assumption of magnetic linearity, the flux linkage and the phase currents are related by:

$$\psi = \mathbf{L}(\theta)\mathbf{i} \tag{12}$$

Then, we can write an augmented system of equations for the SRM in state space form as:

$$\dot{\mathbf{x}}(t) = \begin{pmatrix} \dot{\mathbf{x}}_N(t) \\ \dot{\mathbf{x}}_P(t) \end{pmatrix} = \begin{pmatrix} f_N(t) \\ f_P(t) \end{pmatrix} \begin{pmatrix} \mathbf{x}_N(t) & \mathbf{x}_P(t) \end{pmatrix} + \mathbf{B}\mathbf{u}(t) \tag{13}$$

in which

$$\begin{pmatrix} f_N(t) \\ f_P(t) \end{pmatrix} = [x^T\mathbf{A}_1(t)x + B_1(t)x, \ldots, x^T A_n(t)x + B_n(t)x] \tag{14}$$

and

$$\mathbf{B} = \begin{pmatrix} \mathbf{B}_N \\ 0 \end{pmatrix} \tag{15}$$

where $A_1(t)$, ..., $A_n(t)$ and $B_1(t)$, ..., $B_n(t)$ are real matrix

function, and the subscript N represents the electromagnetic part whereas the subscript P represents the parameter parts of the motor. Assuming the phase currents are measurable, then the output equation will be:

$$\mathbf{y}(t) = \mathbf{C}_N \mathbf{x}_N(t) \tag{16}$$

with

$$\mathbf{C} = [\mathbf{C}_N, 0] \tag{17}$$

Since the augmented motor model combines both the states and the parameters, it is then nonlinear regardless whether the original model is linear or not because of multiplication of states:

$$\begin{aligned} \dot{\mathbf{x}}_N(t) &= f_N(\mathbf{x}_N(t), \theta, \omega) + \mathbf{B}_N \mathbf{u}(t) \\ &= \mathbf{A}_N(\theta, \omega)\mathbf{x}_N(t) + \mathbf{B}_N \mathbf{u}(t) \end{aligned} \tag{18}$$

The load torque T_L is considered as external disturbance and sometimes considered as known or zero [8]. However, as indicated in [19–21], load torque estimation can enhance the overall system performance dramatically. Consequently, T_L was transformed into an unknown and inaccessible state variable and then estimated [19]. Owing to the relatively long time constant of the load when compared to the electromagnetic time constant during a sampling period (= 150μs in this case), we can reasonably assume that the dT_L/dt is zero. Then, we can write a new augmented system of equations combing both the states and the parameters for the SRM in state space form as:

$$\dot{\mathbf{x}}(t) = f(\mathbf{x}(t), \theta, \omega, T_L) + \mathbf{B}\mathbf{u}(t) \tag{19}$$

where the states of the electromechanical part of the system becomes:

$$\mathbf{A}_P(\mathbf{x}_N(t), \theta, \omega, T_L) = \begin{pmatrix} 0 & 0 & 0 & 0 & 0 & 1 & 0 \\ \frac{T_a}{J} & \frac{T_b}{J} & \frac{T_c}{J} & \frac{T_d}{J} & 0 & -\frac{D}{J} & -\frac{1}{J} \\ 0 & 0 & 0 & 0 & 0 & 0 & 0 \end{pmatrix} \tag{20}$$

$$\mathbf{x}_P(t) = [\theta, \omega, T_L]^T \tag{21}$$

4 The full-order extended Luenberger observer

To obtain a linear mathematical model for the SRM, it is assumed that the variables deviate only slightly from state trajectory $\breve{\mathbf{x}}(t)$, then eqn. 14 may be expanded into a Taylor series expansion about this point as follows:

$$\begin{aligned} \dot{\mathbf{x}}(t) =& f(\breve{\mathbf{x}}(t)) + \frac{df}{dx}(\breve{\mathbf{x}}(t))[\mathbf{x}(t) - \breve{\mathbf{x}}(t)] \\ &+ \text{higher order terms} + \mathbf{B}\mathbf{u}(t) \end{aligned} \tag{22}$$

where the derivative df/dx is evaluated at ($\mathbf{x} = \breve{x}$). If the variation ($\mathbf{x} - \breve{x}$) is small, the higher order terms in ($\mathbf{x} - \breve{x}$) may be neglected, then eqn. 25 may be written by donating:

$$\breve{\mathbf{A}}(\breve{\mathbf{x}}) = \frac{df}{dx}(\breve{\mathbf{x}}) \tag{23}$$

as

$$\dot{\mathbf{x}}(t) = f(\breve{\mathbf{x}}(t)) + \breve{\mathbf{A}}(\breve{\mathbf{x}})[\mathbf{x}(t) - \breve{\mathbf{x}}(t)] + \mathbf{B}\mathbf{u}(t) \tag{24}$$

Having obtained a linearised model of the SRM, the linear Luenberger observer theory can directly be used to produce the state estimates of the non-linear model:

$$\dot{\hat{\mathbf{x}}}(t) = f(\breve{\mathbf{x}}(t)) + \breve{\mathbf{A}}(\breve{\mathbf{x}}(t))[\hat{\mathbf{x}}(t) - \breve{\mathbf{x}}] + \mathbf{B}\mathbf{u} + \mathbf{K}(\breve{\mathbf{x}}(t))[\mathbf{y} - \hat{\mathbf{y}}] \tag{25}$$

in which

$$\hat{\mathbf{y}}(t) = \mathbf{C}\hat{\mathbf{x}}(t) \tag{26}$$

If the last estimate is chosen as the operating point for a short sampling time, $\breve{x}$ is conveniently shown as:

$$\breve{\mathbf{x}}(t) = \hat{\mathbf{x}}(t) \tag{27}$$

then eqn. 28 becomes

$$\dot{\hat{\mathbf{x}}}(t) = f(\hat{\mathbf{x}}(t)) + \mathbf{B}\mathbf{u}(t) + \mathbf{K}(\hat{\mathbf{x}}(t))[\mathbf{y}(t) - \hat{\mathbf{y}}(t)] \tag{28}$$

Assuming $\breve{x}$ is equal to the latest estimated value and piecewise constant, then the linear Luenberger observer may be applied within every sampling period. For a choice of:

$$\mathbf{F}(\breve{\mathbf{x}}) = \breve{\mathbf{A}}(\breve{\mathbf{x}}) - \mathbf{K}(\breve{\mathbf{x}})\mathbf{C} \tag{29}$$

$$\mathbf{G}(\breve{\mathbf{x}}) = f(\breve{\mathbf{x}}) - \breve{\mathbf{A}}(\breve{\mathbf{x}})\breve{\mathbf{x}} \tag{30}$$

The FOELO is defined as:

$$\dot{\hat{\mathbf{x}}}(t) = \breve{\mathbf{A}}(\breve{x}, t)\hat{\mathbf{x}}(t) + \mathbf{B}\mathbf{u}(t) + \mathbf{G}(\breve{\mathbf{x}}) + \mathbf{K}\mathbf{C}(\mathbf{x}(t) - \hat{\mathbf{x}}(t)) \tag{31}$$

If the estimation error is shown as:

$$\mathbf{e}(t) = \mathbf{x}(t) - \hat{\mathbf{x}}(t) \tag{32}$$

Then, from eqns. 27 and 28, the error dynamics can be formulated:

$$\dot{\mathbf{e}}(t) = \mathbf{F}(\hat{\mathbf{x}}(t))\mathbf{e}(t) \tag{33}$$

To guarantee the asymptotic behaviour of the error, it is desired to design matrix $\mathbf{F}(\hat{\mathbf{x}}(t))$ in eqn. 36 as a constant matrix $\mathbf{F}$, then it may be rearranged as

$$\dot{\mathbf{e}}(t) = \mathbf{F}\mathbf{e}(t) \tag{34}$$

Eqn. 37 shows that the dynamics of the error can be modified by means of the gain matrix $\mathbf{K}$. If the gain can be designed to place the closed-loop poles of the state error in any desired locations, the system in eqn. 1 is said to be observable [19]. The choice of observer poles is completely arbitrary in principle. The $\mathbf{F}$ can be selected to make the error decay as fast as possible, constrained only by the bandwidth of the available components. In practice, however, it is often difficult to make the observer substantially faster than the system itself. If $\mathbf{K}$ is chosen properly, which guarantees $\mathbf{F}$ is a stable matrix, then $\mathbf{e}$ decays to zero as time proceeds, and $\hat{x}$ converges to $\mathbf{x}$. The rate of convergence is governed by the stability of $\mathbf{F}$. If $\mathbf{F}$ is time invariant, then it is stable if and only if its eigenvalues all have negative real parts. These eigenvalues determine the rate of convergence of the observer.

In eqn. 34 matrix $\mathbf{K}$ is the observer gain used to specify the given pole locations. The values of $\mathbf{K}$ for the continuous case were obtained using the command PLACE implemented in MATLAB [22]. For this case the results obtained from it for the $\mathbf{F}_N$ were very interesting yielding the following relationship:

$$\mathbf{K}_N = \lambda_n^* \mathbf{L}_n - \mathbf{R} \tag{35}$$

where λ_n is the estimate pole. This relationship was tested using simulation for the discrete-time model to find the optimal gain matrix $\mathbf{K}$. Therefore, for an online implementation, a simplified method for the gain matrix and lower computation cost was established.

4.1 Discrete-time full-order extended Luenberger observer

Up to now, the observer theory, which was derived, was in continuous-time form. If we want to implement the observer by the use of digital computer, we must convert a continuous-time system to a discrete-time system. In this case, state estimation would be one function of an overall digital control scheme. To do this, one important condition, is that the discrete-time solutions must be valid at equally spaced sampling

instants. In discretising the continuous time system, it is assumed that the inputs change only at these same instants. The linear discrete-time system can be written in the following form of the vector matrix difference equation:

$$\mathbf{x}(k+1) = \Phi\mathbf{x}(k) + \Gamma\mathbf{u}(k) \tag{36}$$

$$\hat{\mathbf{x}}(k+1) = \Phi(k)\hat{\mathbf{x}}(k) + \Gamma(k)\mathbf{u}(t) + \zeta(k) + \mathbf{K}[\mathbf{y}(k) - \xi\hat{\mathbf{x}}(k)] \tag{37}$$

where $\mathbf{x}(k)$ represents the present state and $\mathbf{x}(k+1)$ represent the next state and t_s is the sampling interval. Although eqn. 37 is linear and time invariant in a sampling period, since it is updated in each of the sampling instants it is virtually nonlinear, and time varying over the whole time axis. This suggests a reality that the discretisation must be done in every sampling interval.

5 Simulation results of the full-order extended Luenberger observer

The analysis of the observer performance from an analytical point of view is very difficult owing to the nonlinear time-varying characteristics of the algorithm. In this Section the performance of the observer will be investigated by simulations assuming that the parameter values used in synthesising the observer agree with the actual values. Special attention will be paid to understand its tracking capabilities and performance under different working conditions. The simulation results are shown in Figs. 1–6. The results show that the algorithm exhibits a good tracking performance for speed and parameter variations.The FOELO covers all the state variables and the parameters of the system which is of the order of seven. The effect of the pole position on the observer performance has been investigated extensively. Since the full-order observer was considered, it has a set of poles which is seven. The first four poles are those associated with the phase flux estimates, the fifth pole is that associated with the rotor position estimate, the sixth is that associated with the speed estimate and the seventh is that associated with the load torque estimate. Throughout the analysis of the full-order observer, the poles of the observer were changed deliberately to test how the performance of the observer varied.

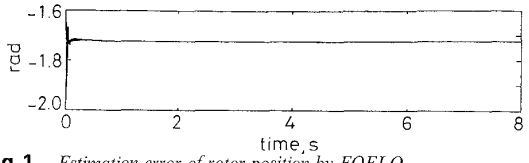

Fig. 1 *Estimation error of rotor position by FOELO*
Initial conditions are $\hat{\theta}(0) = \pi/2$ rad, $\hat{\omega}(0) = 0.3$ rad/s, $\hat{T}_L(0) = 0$
Poles: a = [–200 –200 –200 –200 –20 –10 –1], b = [–200 –200 –200 –200 –20 –50 –1] c = [–200 –200 –200 –200 –20 –100 –1]

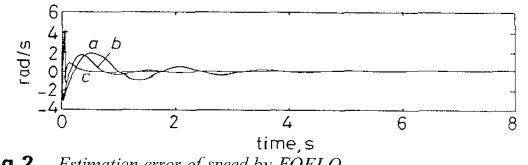

Fig. 2 *Estimation error of speed by FOELO*
Initial conditions are $\hat{\theta}(0) = \pi/2$ rad, $\hat{\omega}(0) = 0.3$ rad/s, $\hat{T}_L(0) = 0$
Poles: a = [–200 –200 –200 –200 –20 –10 –1], b = [–200 –200 –200 –200 –20 –50 –1] c = [–200 –200 –200 –200 –20 –100 –1]

Figs. 1–3 illustrate the simulation results of the full-order observer when the motor was running with no load from standstill. To test the behaviour of the observer, choosing untrue initial conditions of $\hat{\theta}(0) = \pi/2$ rad, $\hat{\omega}(0) = 0.3$ rad/s and $\hat{T}_L(0) = 0$. For this simulation the pole associated with the rotor position estimate was change whilst keeping the rest constant, which are: a = [–200 –200 –200 –200 –20 –10 –1], b = [–200 –200 –200 –200 –20 –50 –1], c = [–200 –200 –200 –200 –20 –100 –1].

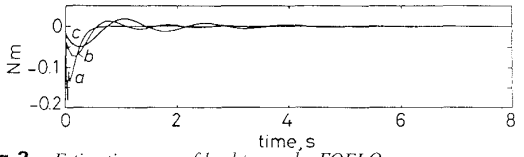

Fig. 3 *Estimation error of load torque by FOELO*
Initial conditions are $\hat{\theta}(0) = \pi/2$ rad, $\hat{\omega}(0) = 0.3$ rad/s, $\hat{T}_L(0) = 0$
Poles: a = [–200 –200 –200 –200 –20 –10 –1], b = [–200 –200 –200 –200 –20 –50 –1] c = [–200 –200 –200 –200 –20 –100 –1]

Figs. 1–3 show that the pole positions of the state estimate have again clear influence on the convergence rate of the estimated values. It is observed as expected that the bias is less effective at steady state. It is also observed that as the poles go more to the left, the convergence becomes faster. It was also noticed that the rotor position estimate cannot reduce the initial error to the zero itself without help of an external marker [7,8]. This is probably common for position estimation on any kind of motors.

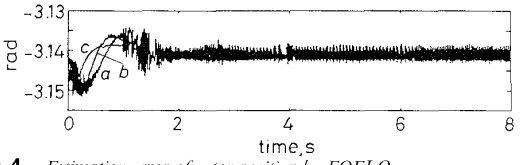

Fig. 4 *Estimation error of rotor position by FOELO*
Initial conditions are $\hat{\theta}(0) = \pi$rad, $\hat{\omega}(0) = 0.3$ rad/s, $\hat{T}_L(0) = 0$
Poles: a = [–200 –200 –200 –200 –20 –10 –1], b = [–200 –200 –200 –200 –20 –50 –1] c = [–200 –200 –200 –200 –20 –100 –1]

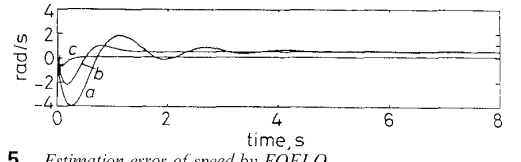

Fig. 5 *Estimation error of speed by FOELO*
Initial conditions are $\hat{\theta}(0) = \pi$rad, $\hat{\omega}(0) = 0.3$ rad/s, $\hat{T}_L(0) = 0$
Poles: a = [–200 –200 –200 –200 –20 –10 –1], b = [–200 –200 –200 –200 –20 –50 –1] c = [–200 –200 –200 –200 –20 –100 –1]

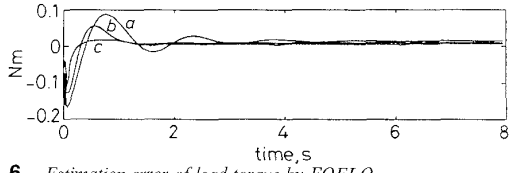

Fig. 6 *Estimation error of load torque by FOELO*
Initial conditions are $\hat{\theta}(0) = \pi$rad, $\hat{\omega}(0) = 0.3$ rad/s, $\hat{T}_L(0) = 0$
Poles: a = [–200 –200 –200 –200 –20 –10 –1], b = [–200 –200 –200 –200 –20 –50 –1] c = [–200 –200 –200 –200 –20 –100 –1]

Figs 4–6 show the simulation results with the initial conditions of $\hat{\theta}(0) = \pi$ rad, $\hat{\omega}(0) = 0.3$ rad/s, $\hat{T}_L(0) = 0$. As seen from the Figures, the bias at steady state becomes significant and rotor position estimate is rather noisy.

Figs. 7–9 show the simulation results with the initial conditions of $\hat{\theta}(0) = 3\pi/2$ rad, $\hat{\omega}(0) = 0.3$ rad/s, $\hat{T}_L(0) = 0$. The general trends of these results are almost identical with Figs. 4–6. The simulation was run with the initial conditions of $\hat{\theta}(0) = 0$, $\hat{\omega}(0)$, = 50 rad/s, $\omega(0) = 70$ rad/s, $\hat{T}_L(0) = 0$ with a set of poles of [–100 –100 –100 –

100 –20 –10 –1] while the motor at the steady state with no load as shown in Figs. 10–12. It is observed that the observer has good tracking capabilities and transient performance.

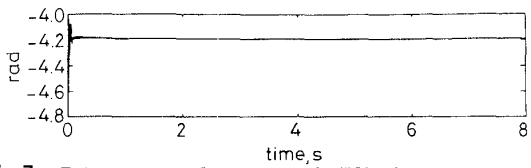

Fig. 7 *Estimation error of rotor position by FOELO*
Initial conditions are $\theta(0) = 3\pi/2$rad, $\hat{\omega}(0) = 0.3$ rad/s, $\hat{T}_L(0) = 0$
Poles: a = [–200 –200 –200 –200 –20 –10 –1], b = [–200 –200 –200 –200 –20 –50 –1] c = [–200 –200 –200 –200 –20 –100 –1]

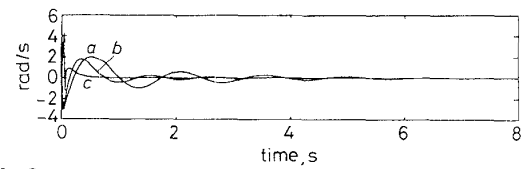

Fig. 8 *Estimation error of speed by FOELO*
Initial conditions are $\theta(0) = 3\pi/2$rad, $\hat{\omega}(0) = 0.3$ rad/s, $\hat{T}_L(0) = 0$
Poles: a = [–200 –200 –200 –200 –20 –10 –1], b = [–200 –200 –200 –200 –20 –50 –1] c = [–200 –200 –200 –200 –20 –100 –1]

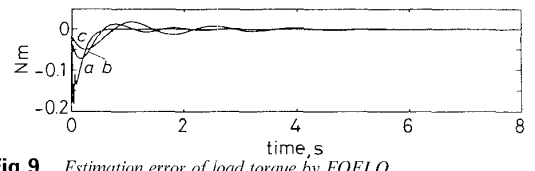

Fig. 9 *Estimation error of load torque by FOELO*
Initial conditions are $\theta(0) = 3\pi/2$rad, $\hat{\omega}(0) = 0.3$ rad/s, $\hat{T}_L(0) = 0$
Poles: a = [–200 –200 –200 –200 –20 –10 –1], b = [–200 –200 –200 –200 –20 –50 –1] c = [–200 –200 –200 –200 –20 –100 –1]

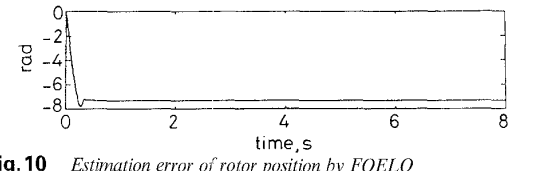

Fig. 10 *Estimation error of rotor position by FOELO*
Initial conditions are $\theta(0) = 0$, $\hat{\omega}(0) = 50$rad/s, $\omega(0) = 70$rad/s, $\hat{T}_L(0) = 0$
Poles: = [–100 –100 –100 –100 –20 –10 –1]

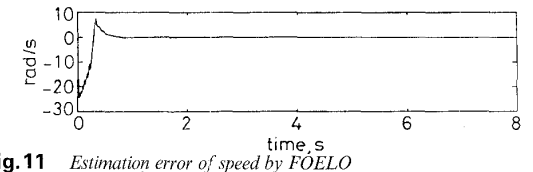

Fig. 11 *Estimation error of speed by FOELO*
Initial conditions are $\theta(0) = 0$, $\hat{\omega}(0) = 50$ rad/s, $\omega(0) = 70$ rad/s, $\hat{T}_L(0) = 0$
Poles: = [–100 –100 –100 –100 –20 –10 –1]

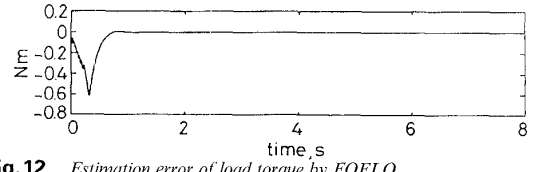

Fig. 12 *Estimation error of load torque by FOELO*
Initial conditions are $\theta(0) = 0$, $\hat{\omega}(0) = 50$ rad/s, $\omega(0) = 70$ rad/s, $\hat{T}_L(0) = 0$
Poles: = [–100 –100 –100 –100 –20 –10 –1]

The above simulations were run while the motor was working under no load. The results shown in Figs. 13–15 were obtained whilst the motor operated under a constant load of 0.1 Nm. The initial conditions of $\hat{\theta}(0) = \pi/2$ rad, $\hat{\omega}(0) = 0.3$ rad/s and $\hat{T}_L(0) = 0.1$ Nm were used with three different poles for the speed. It is noticed that the observer behaves well under load condition, too. However, the steady state bias exists in the speed and load torque estimations.

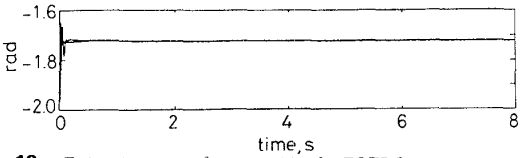

Fig. 13 *Estimation error of rotor position by FOELO*
Initial conditions are $\theta(0) = \pi/2$ rad, $\hat{\omega}(0) = 0.3$ rad/s, $\hat{T}_L(0) = 0.1$ Nm
Poles: a = [–200 –200 –200 –200 –20 –10 –1], b = [–200 –200 –200 –200 –20 –50 –1] c = [–200 –200 –200 –200 –20 –100 –1]

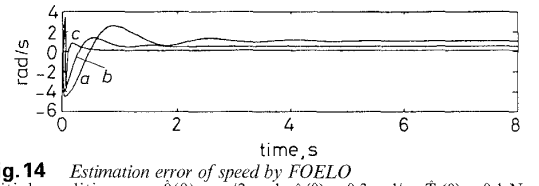

Fig. 14 *Estimation error of speed by FOELO*
Initial conditions are $\theta(0) = \pi/2$ rad, $\hat{\omega}(0) = 0.3$ rad/s, $\hat{T}_L(0) = 0.1$ Nm
Poles: a = [–200 –200 –200 –200 –20 –10 –1], b = [–200 –200 –200 –200 –20 –50 –1] c = [–200 –200 –200 –200 –20 –100 –1]

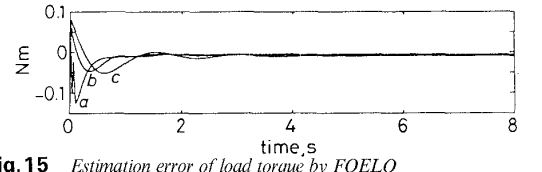

Fig. 15 *Estimation error of load torque by FOELO*
Initial conditions are $\theta(0) = \pi/2$ rad, $\hat{\omega}(0) = 0.3$ rad/s, $\hat{T}_L(0) = 0.1$ Nm
Poles: a = [–200 –200 –200 –200 –20 –10 –1], b = [–200 –200 –200 –200 –20 –50 –1] c = [–200 –200 –200 –200 –20 –100 –1]

For an increased initial condition of rotor position error, the result shown in Figs. 16–18, the observer still behaves well, though with increased noise.

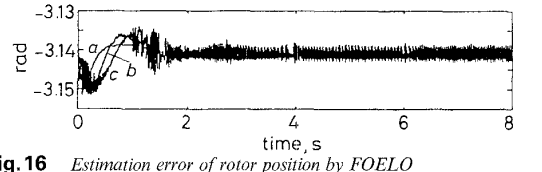

Fig. 16 *Estimation error of rotor position by FOELO*
Initial conditions are $\theta(0) = \pi$ rad, $\hat{\omega}(0) = 0.3$ rad/s, $\hat{T}_L(0) = 0.1$ Nm
Poles: a = [–200 –200 –200 –200 –20 –10 –1], b = [–200 –200 –200 –200 –20 –50 –1] c = [–200 –200 –200 –200 –20 –100 –1]

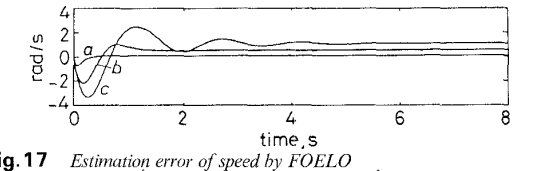

Fig. 17 *Estimation error of speed by FOELO*
Initial conditions are $\theta(0) = \pi$ rad, $\hat{\omega}(0) = 0.3$ rad/s, $\hat{T}_L(0) = 0.1$ Nm
Poles: a = [–200 –200 –200 –200 –20 –10 –1], b = [–200 –200 –200 –200 –20 –50 –1] c = [–200 –200 –200 –200 –20 –100 –1]

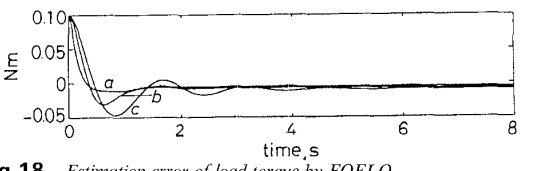

Fig. 18 *Estimation error of load torque by FOELO*
Initial conditions are $\theta(0) = \pi$ rad, $\hat{\omega}(0) = 0.3$ rad/s, $\hat{T}_L(0) = 0.1$ Nm
Poles: a = [–200 –200 –200 –200 –20 –10 –1], b = [–200 –200 –200 –200 –20 –50 –1] c = [–200 –200 –200 –200 –20 –100 –1]

6 Practical set-up

The observer was implemented using a TMS320C30 32 bit DSP. The structure of the complete system is shown in Fig. 19. The motor is driven by a split DC source MOSFET converter. The position and speed observer are evaluated experimentally using a four-phase SR motor with six rotor poles and eight stator poles (for more details see the Appendix). The DSP used supports 32 bit floating point multiplication with a clock frequency of 30MHz. The DSP computes not only the observer algorithm but also deals with the phase current chopping and switching pattern for the drive. The estimated position is used for the operation of the drive. The observer was run online at a sampling rate of 150μs. The drive system was equipped with an incremental shaft encoder to provide position and speed measurements for comparison purposes.

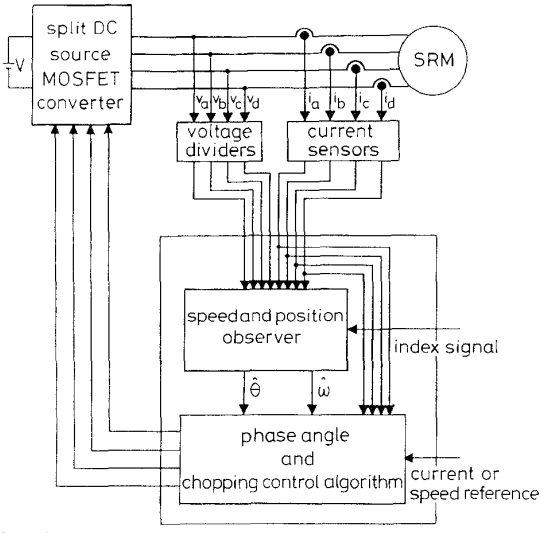

Fig. 19 *Structure of complete system*

A differential voltage information for each phase was taken directly measured across each winding with the required buffering circuitry. A voltage divider network was constructed for each side of each phase using precision resistors. The phase currents are measured by Hall-effect sensors model of RS 257–436 that can output a 0 – ±10V instantaneous voltage corresponding to the phase current.

The Luenberger observer is deterministic which means that the system is not affected from the external disturbance and the noise, thus special attention should be paid for preventing these unwanted signals. Noise and out-of-band input signals were prevented from folding over the signal bandwidth of interest by employing some form of presampling filter, often called an antialiasing filter.

7 Practical results of the full-order extended Luenberger observer

The estimator simulations presented earlier were helpful to understand and predict the performance of the observer. Consequently, it was necessary to evaluate and test the algorithms in an actual working conditions.

The practical estimation results shown were obtained while the observer was running in a closed-loop environment as shown in Fig. 20. It means that once the rotor position is estimated, it is immediately used for controlling the phase switching. That is to say, the shaft position encoder was replaced by the observer. Therefore, the whole system would be affected if there is any steady state or transient error which will be imposed to the observer itself by the converter outputs.

The practical position sensorless operation of the drive has been tested using the estimated position and speed values obtained from the observers. To avoid magnetic non linearity, the motor was operated in the linear region. The drive operation has been tested when step changes take place in the load torque T_L as well as when the observer was running from an unknown initial position at standstill similar to the case when an incremental shaft encoder is used.

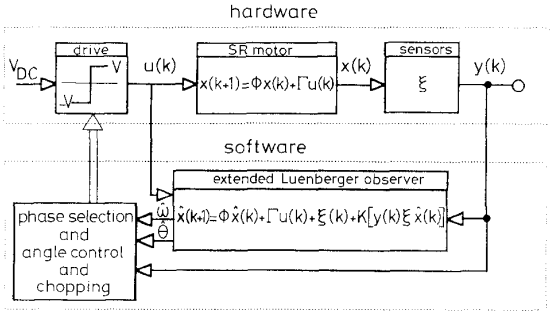

Fig. 20 *Mathematical representation of complete system*

As mentioned previously, initially the pole placement was done using MATLAB's PLACE command which is an implementation of the Ackerman's formula to calculate gains [22]. Although this command could be written in the C programming language for the online implementation, it is rather complicated. During the simulation stage, it was felt that the gain did not require a robust calculation mechanism. Therefore, a simplified method based upon eqn. 35 for the pole placement was established.

Figs. 21–23 show the results while the motor was running at a speed of 105 rad/s at steady state.

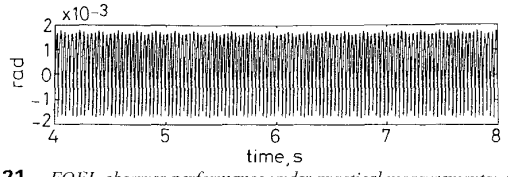

Fig. 21 *FOEL observer performance under practical measurements: estimation error of rotor position*

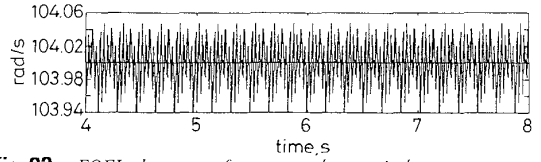

Fig. 22 *FOEL observer performance under practical measurements: estimation of speed*

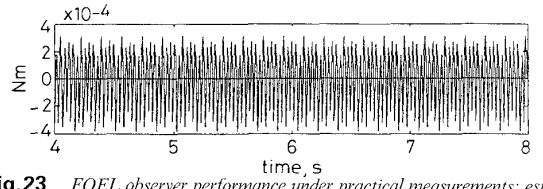

Fig. 23 *FOEL observer performance under practical measurements: estimation of load torque*

Figs. 24–26 demonstrate the results when step changes take place in the load torque T_L with the motor running at high speed. During this phase, the load torque of 0.1 Nm was applied to the motor, which causes the transients to appear. The measured and estimated speed shows that observer tracking speed is very high and the $\hat{\omega}$ catches the ω.

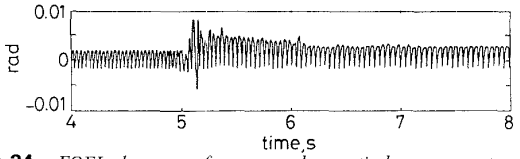

Fig. 24 *FOEL observer performance under practical measurements: estimation error of rotor position*

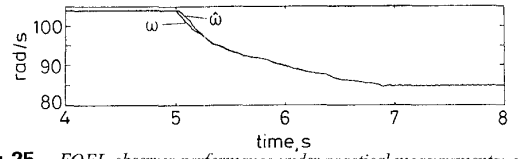

Fig. 25 *FOEL observer performance under practical measurements: estimation of speed*

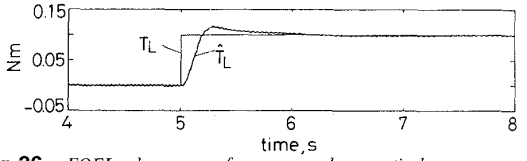

Fig. 26 *FOEL observer performance under practical measurements: estimation of load torque*

Figs. 27–29 present the results obtained while the motor was running at a speed of 67 rad/s. The motor was loaded with sudden load torque of 0.1 Nm which is the half of the rated load value.

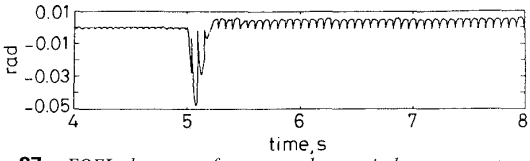

Fig. 27 *FOEL observer performance under practical measurements: estimation error of rotor position*

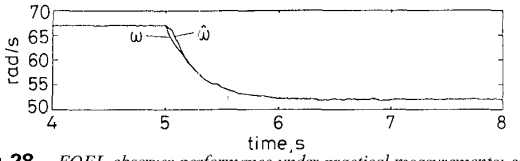

Fig. 28 *FOEL observer performance under practical measurements: estimation of speed*

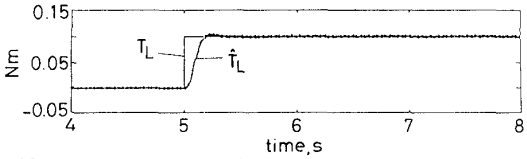

Fig. 29 *FOEL observer performance under practical measurements: estimation of load torque*

Figs. 30–32 show the results for the starting-up transients.

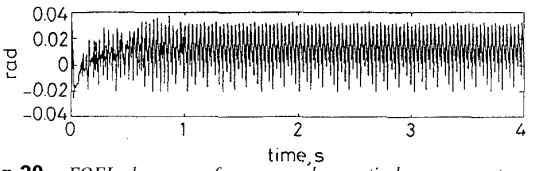

Fig. 30 *FOEL observer performance under practical measurements: estimation error of rotor position*

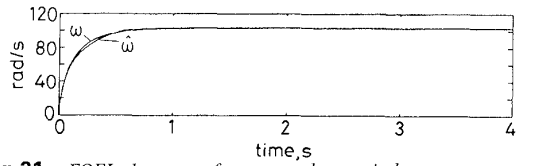

Fig. 31 *FOEL observer performance under practical measurements: estimation of speed*

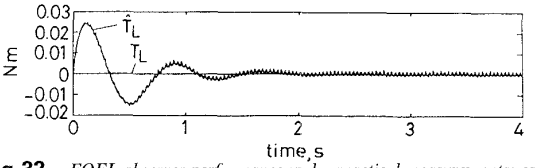

Fig. 32 *FOEL observer performance under practical measurements: estimation of load torque*

7.1 Some remarks about the observer implementation

In general, the problems and important points for the implementation of the observer are listed as follow:

- The convergence rate is highly affected by initial conditions. Generally, the algorithm converges to its true values very fast. However, transient behaviour is poor if the initial conditions contained a large error and large over shoots take place.
- The poles can be placed in such a position that estimated values converge fast to their true values faster.
- The algorithm converges to the true values in steady state whilst during transient conditions the estimated values are close to true values.
- In general the FOEL observer exhibits better performance than the ROEL observer since the former covers the whole states of the system.
- As load torque was transformed into an unknown and inaccessible state variable, the overall system performance was improved dramatically.
- Since the Luenberger observer is a deterministic observer, noisefree measurement should be ensured.

8 Conclusions

In this paper, an observer algorithm based upon the extended Luenberger observer theory, which estimates all the electromagnetic and electromechanical states, has been developed. These include plant nonlinearities which naturally lead to an estimator with improved performance over the existing estimation schemes.

The experimental configuration has also been discussed and the performance of the switched reluctance motor drive operating with the estimated values has been analysed. Some important problems and points for the implementation of the observer have been pointed out.

It is possible to extend and make improvements to the present observer model. The modelling of the

inductance variation is a very difficult task and therefore, an adaptive observer that could follow variations in the inductance would be a very useful feature. The present observer algorithm could be modified so it is extended with an online parameter identification based on other state variables such as voltage and current. This would give the system the freedom to work in a much wider range of circumstances (i.e. within the saturation region as well as the linear region). However, the added complexity would have to be carefully examined to assess the effects on the practical implementation, in particular, sampling frequency and noise introduced by the observed quantities.

9 References

1 LAWRENSON, P.J., STEPHENSON, J.M., BLENKINSOP, P.T., CORDA, J., and FULTON, N.N.: 'Variable switched reluctance motors', *IEE Proc. B*, 1980, **127**, (4), pp. 253–265

2 ACARNLEY, P.P., ROLAND, J.H., and HOOPER, C.W.: 'Detection of rotor position in stepping and switched reluctance motors by monitoring of current waveforms', *IEEE Trans.*, 1985, **IE–32**, (3), pp. 215–222

3 BASS, J.T., EHSANI, M., and MILLER, T.J.E.: 'Robust torque control of switched reluctance motor without shaft position sensor', *IEEE Trans.*, 1986, **IE–33**, (3), pp. 212–216

4 BASS, J.T., EHSANI, M., and MILLER, T.J.E.: 'Simplified electronics for torque control of sensorless switched reluctance motor', *IEEE Trans.*, 1987, **IE–34**, (2), pp. 234–239

5 PANDA, S.K., and AMARATUNGA, G.A.J.: 'Waveform detection technique for indirect rotor position sensing of switched reluctance motor drives Part 1: analysis', *IEE Proc. B*, 1993, **140**, pp. 80–88

6 PANDA, S.K., and AMARATUNGA, G.A.J.: 'Waveform detection technique for indirect rotor position sensing of switched reluctance motor drives Part 2: experimental results', *IEE Proc. B*, 1993, **140**, pp. 89–96

7 RAY, W.F., and AL-BAHADLY, I.H.: 'Sensorless methods for determining the rotor position of switched reluctance motors', European Power Electronics '93, Brighton, UK, 1993, Vol. 6, pp. 7–13

8 LUMSDAINE, A., and LANG, J.H.: 'State observer for variable reluctance motors', *IEEE Trans.*, 1990, **IE–37**, (2), pp. 133–142

9 ELMAS, C. and ZELAYA DE LA PARRA, H.: 'Position sensorless operation of a switched reluctance drive based on observer', European Power Electronics '93, Brighton, UK, 1993, Vol. 6, pp. 82–87

10 TAJIMA, H., and HORY, H.: 'Speed sensorless field orientation control of the induction machine', *IEEE Trans. Ind. Appl.*, 1993, **29**, (1), pp. 175–180

11 FURUHASHY, T., SANGWONGWANICH, S., and OKUMA, S.: 'A position and velocity sensorless control for brushless DC motors using an adaptive sliding mode observer', *IEEE Trans.*, 1992, **IE–39**, (2), pp. 89–95

12 GARCIA–CERRADA, A.: Observer-based field-oriented controller for an inverter-fed traction induction motor drive, Ph.D. Thesis, School of Electronic and Electrical Engineering, University of Birmingham, England, 1990

13 LUENBERGER, D.G.: 'Observers for multivariable system', *IEEE Trans. Autom. Control*, 1966, **11**, (2), pp. 190–197

14 KALMAN, R.E., and BUCY, R.S.: 'New results in linear filtering and prediction theory', *Trans. ASME, D, J. Basic Eng.*, 1961, pp. 95–108

15 ORLOWSKA-KOWALSKA T.: 'Application of extended Luenberger observer for flux and rotor time constant estimation in induction motor drives', *IEE Proc. D*, 1989, **136**, (6), pp. 324–330

16 LUENBERGER, D.G.: 'An introduction to observers', *IEEE Trans. Autom. Control*, 1971, **16**, (6), pp. 596–602

17 KRISHNAN, R., ARUMUGAM, R., and LINDSAY, J.F.: 'Design procedure for switched reluctance motors', *IEEE Trans. Ind. Appl.*, 1988, **24**, (3), pp. 216–226

18 MILLER, T.J.E., and MCGILP, M.: 'Nonlinear theory of the switched reluctance motor for rapid computer aided design', *IEE Proc. B*, **137**, (6), pp. 337–347

19 MLANOVIC, M., and JEZERNIK, K.: 'Estimation of parameters and load torque of a thyristor driven DC motor drive'. European Power Electronics '89, Aachen, Germany, 1989, Vol. 6, pp. 1345–1349

20 BRDYS, M.A., and DU, T.: 'Algorithms for joint state and parameter estimation in induction motor drive systems'. International conference on *Control* '91, 1991, Vol. 2, pp. 915–920 (IEE Conf. Publ. 332)

21 VON WESTERHOLT, E., PIETRZAK-DAVID, M., and DE FORNEL, B.: 'Extended state estimation of nonlinear modeled induction machines'. Power Electronics Specialist conference, Toledo, Spain, June–July 1992, Vol. 1, pp. 271–278

22 FRANKLIN, G.F., POWELL, J.D., and WORKMAN, M.L.: 'Digital control of dynamic systems' (Addison–Wesley Publishing Company, Inc., 1990)

Appendix

Motor power = 1 kW

4 phase

Stator poles = 8

Rotor poles = 6

$R = 2.9\Omega$

$B = 0.0027\,\text{Nms}$

$J = 0.00029\,\text{Nms}^2$

The DC input voltage of the inverter = 120 V.